



Copyright © 2019 American Scientific Publishers All rights reserved Printed in the United States of America Journal of Biomedical Nanotechnology Vol. 15, 363–372, 2019 www.aspbs.com/jbn

Using Plant Virus Based Nanorods to Modulate the Differentiation of Human Bone Marrow Stem Cells

Tao Liu^{1,†}, Xia Zhao^{2,†}, Lei Wang¹, Jia Yang^{3,4}, Kamolrat Metavarayuth³, Yuan Lin², Jishan Yuan^{1,*}, and Qian Wang^{3,*}

Tobacco mosaic virus (TMV) is a protypical nanorod-shaped bioparticles that has been used as a building block to construct a variety of self-assembled nanomaterials for different biomedical applications, including drug delivery, *in vivo* imaging, tumor immunotherapy and tissue engineering. In this work, the roles of TMV and its mutant TMV-RGD1 nanoparticles on the differentiation of human bone marrow stem cells (hBMSCs), an important process in bone regeneration, were carefully investigated. We observed that cells cultured on the TMV-RGD1 nanorods coated substrate showed significantly higher levels of gene and protein expression of osteo-specific markers osteocalcin (OCN) and bone morphogenetic protein 2 (BMP2). Investigation of alkaline phosphatase (ALP) activity and calcium deposition further confirmed that the TMV-RGD1 substrate could promote the osteogenesis and induce the mineralization of hBMSCs. On the other hand, the adipogenesis was downregulated on TMV and TMV-RGD1 coated substrates. Taken together, this study demonstrates for the first time the potential of TMV-RGD1 in promoting osteogenic differentiation of hBMSCs which can lead to future applications in clinical bone engineering.

KEYWORDS: Bionanoparticle, Multivalency, Nanotopography, Human Bone Mesenchymal Stem Cells, Osteogenic Differentiation.

INTRODUCTION

Bone marrow derived mesenchymal stem cells (BMSCs) are the most well-known multipotent cells which have the ability to differentiate into various lineages, including osteoblasts, chondrocytes and adipocytes, etc.¹⁻³ The differentiation potential of BMSCs makes it a good candidate for regenerative therapies in the field of bone or cartilage regeneration.^{4,5} The differentiation of BMSCs relies on many factors, including physical, chemical and biological cues present in the stem cell microenvironments. In addition, the surface chemistry and topography of materials also play a crucial role in regulating the cellular differentiation of BMSCs.⁶⁻⁹ Therefore, understanding the specific

cellular behaviors of BMSCs on a given substrate is the key to apply BMSCs to tissue engineering in the clinic.

Many reports have confirmed that a variety of organic and inorganic nanoparticles could accelerate the osteogenic differentiation of BMSCs, such as hydroxyapatite nanoparticles and gold nanoparticles. 10-15 Plant viral nanoparticles are emerging as promising building blocks for improving osteogenic differentiation of stem cells. 16-19 In particular, Tobacco mosaic virus (TMV) is 300 nm in length with a diameter of 18 nm, which resembles the structure of major extra cellular matrix (ECM) components. The viral capsid of TMV consists of 2130 coat protein units which assemble into the rod-like helical structure. Due to the known chemical and biological properties, it is feasible to functionalize TMV nanorods using chemical and genetic modification methods.^{20,21} For example, it was reported that the genetically modified TMV-RGD1 mutant with multivalent display of cell adhesion motifs arginine-glycine-aspartic acid (RGD)

Received: 21 August 2018 Accepted: 25 October 2018

¹ Department of Orthopaedic Surgery, The Affiliated First People's Hospital to Jiangsu University, Zhenjiang, Jiangsu 212002, P. R. China

² State Key Laboratory of Polymer Physics and Chemistry, Changchun Institute of Applied Chemistry, Chinese Academy of Sciences, 5625 Renmin Street, Changchun, Jilin 130022, P. R. China

³ Departments of Chemistry and Biochemistry, University of South Carolina, Columbia, SC 29208, United States

⁴ MicroSep, LLC, 85 Shashan Road, Suit B219, Jiangyin, Jiangsu 214400, P. R. China

^{*}Authors to whom correspondence should be addressed. Emails: jishan0926@hotmail.com, wang263@mailbox.sc.edu

[†]These two authors contributed equally to this work.

could accelerate cell adhesion and spreading in serumfree osteogenic media.^{22,23} Since the BMSCs derived from human (hBMSCs) hold tremendous promise for in clinic application, it is important to explore the effect of TMV nanoparticles on the differentiation of hBMSCs.

It is well-known that human MSCs respond differently from rodent MSCs to osteoinductive conditions.²⁴ For instance, BMPs induce osteogenesis in MSC derived from rats and mice. However, it is relatively inefficient in inducing human MSC to undergo osteogenesis.²⁵ In another study, Reilly and co-workers found that human MSCs and rat MSCs respond differently to bioactive glass.²⁶ Rat MSCs showed elevated levels of alkaline phosphatase activity when grown on 45S5 bioactive glass, whereas human MSCs produced markedly less alkaline phosphatase activity, and did not respond to the growth factor BMP2 in the same way as rat MSCs. In another example, we have reported that topographies created by Potato virus X (PVX) coated substrates enhanced osteogenic differentiation of rat BMSCs as indicated by the upregulation of osteogenic markers and increase of calcium deposition;²⁷ in contrast, Commandeur group's study did not observe an increase of calcium deposition of human MSCs cultured on PVX coated substrates.²⁸

Therefore, to better utilize TMV as building block for regenerative therapy in the clinic, we investigated how the differentiation of hBMSCs would be influenced by TMVcoated substrates. For the first time our work demonstrates that the topography and multivalent ligand display general 10 μ g/mL insulin, 200 μ M indomethacin and 0.5 μ M erated by TMV and its mutant TMV-RGD1 have great 3-isobutyl-1-methylxanthine (IBMX). After induction for impacts on the differentiation process of hBMSCs.

METHODS

Virus Purification

Wild type TMV and its mutant TMV-RGD1 nanoparticles were purified from infected leaves according to previously reported method.²³ The structure of TMV and TMV-RGD1 were characterized by transmission electron microscopy (TEM) analysis. Briefly, TEM analysis was carried out by dropping 20 µL aliquots of each sample at a concentration of 0.1 mg/mL onto 300-mesh carbon-coated copper grids. Then the grids were viewed with JEOL JEM-1011 microscope.

Preparation of Virus-Coated Substrates

Viruses based substrates were prepared according to a protocol previously reported.²⁷ Briefly, 12-well tissue culture plates (TCPs) were first coated with 0.1 mg/mL polyd-lysine (PDL). 0.7 mL of 1 mg/mL TMV or TMV-RGD1 in 18.2 m Ω water were dropped into PDL coated plate and incubated under sterile cells culture hood for overnight. The bottoms of each well were rinsed briefly with 18.2 m Ω water before used for cell culture. The surface morphology of virus based substrates were characterized by atomic force microscopy (AFM). The bottoms of each virus coated 12-well plate were cut out and observed by a Bruker Multimode 8 SPM.

Human Bone Marrow Stem Cells (hBMSCs) Isolation and Expansion

Human bone marrow cells were harvested from healthy patients undergoing hip and knee arthroplasty as previously described.²⁹ The hBMSCs were isolated and used in accordance with the guidelines for human tissue experimentation by the Affiliated First People's Hospital to University of Jiangsu, Zhenjiang, China. Briefly, marrow cells were aspirated from the femoral medullary cavity. The aspirate was washed and resuspended in basal media, then centrifuged at 1500 rpm for 10 min. The pellet was resuspended in medium and overlaid on a Ficoll gradient, then centrifuged at 1500 rpm for 45 min to concentrate cells at interface layer. The cells were collected and washed with DMEM medium, then transferred in growth DMEM containing 10% FBS and incubated at 37 °C with 5% humidified CO₂. The non-adherent cells were removed after 24 hours and the remaining adherent cells were cultured for further experiments. To induce osteogenesis, growth media were replaced with osteogenic media consisting of DMEM supplemented with 10% FBS, 100 nM dexamethasone, 1 mM sodium β -glycerophosphate and 50 μM vitamin C. To induce adipogenesis, growth media were replaced with adipogenic media consisting of DMEM supplemented with 10% FBS, 1 μM dexamethasone, 3 days, the medium was changed to growth media containing 10 μ g/mL insulin. Media were replenished every 3 days.

Cell Morphology and Proliferation

TCP and virus coated substrates were seeded with hBMSCs in osteogenic DMEM and allowed to culture for various periods. The cells morphology on the tests were examined by inverted microscope. MTT test was carried out to investigate the cell adhesion and proliferation of hBMSCs grown on the virus coated substrates. Briefly, after culture for 6 h, 4 d, 7 d, 14 d, cells were incubated for another 4 h in MTT (0.5%) containing DMEM, then the medium was carefully removed. 150 μ L/well dimethyl sulfoxide was added and oscillated gently to make crystal dissolved. The absorbance at 492 nm was measured using a microplate reader.

Real-Time Quantitative Polymerase Chain Reaction (RT-qPCR) Analysis

hBMSCs were seeded on TCP and virus coated substrates and allowed to attach overnight in growth media. The media were replaced to osteogenic media and cultured for 6 h, 4 d, 7 d, and 14 d. The cell culture were terminated at each time point and total RNA was subsequently

extracted from cells using RNAiso plus (Takara) according to the manufacturer's instructions. The total RNA was reverse-transcribed into cDNA using an M-MLV Reverse Transcriptase kit (Invitrogen), and the resultant cDNA mixture was diluted 10 fold in RNase free ddH2O. RTqPCR amplification was performed using SYBR Premix Ex TaqTM kit (Takara) in a 20 μ L reaction containing $0.4~\mu L$ of each primer, $0.4~\mu L$ ROX Reference Dye and 2 μL of cDNA. The PCR primers were GCACCAAGAT-GAACACAG and GAGCCACAATCCAGTCAT for bone morphogenetic protein 2 (BMP2), AGCGAGGTAGT-GAAGAGAC and GAAAGCCGATGTGGTCAG for osteocalcin (OCN), CCAATGATGAGAGCAATGAG and GTCTACAACCAGCATATCTTC for osteopontin (OPN), CAGACACGACAACATCCTA CTAGCCTCAand GAGCCAGAT for TGF-β, CAGCACTCCATATCTC-TACTAT and CTTCCATCAGCGTCAACA for RunX2, GCCAACTATGCCTCTCAG and AGAACAGTGTAAGT-GAACCT for Collagen I, GCTGGATGAGAACAACAC and AAGAAGTGGCAGGAAGAG for osteonectin, AGC-GAGCATCCCCCAAAGTT and GGGCACGAAGGCT-CATCATT for β -actin. RT-qPCR was carried out on a ABI 7500 Fast (Applied Biosystems) with following program: 95 °C for 30 sec followed by 40 cycles of 95 °C for 5 sec and 58 °C for 34 sec. The relative gene expression level was calculated with $2-\Delta\Delta Ct$ method using β -actin as internal control.

Immunohistochemical Staining Copyright: American

The localization of osteogenic markers OCN, OPN and BMP2 were analyzed by immunohistochemical staining. hBMSCs culture on TCP, TMV and TMV-RGD1 coated substrates were terminated on 6 h, 4 d and 7 d. Cells were fixed with 4% formaldehyde in phosphate-buffered saline (PBS) containing 1% sucrose at 37 °C for 15 min. The fixative was then removed and the samples were permeabilized with 0.1% of Triton-X 100 at 4 °C for 10 min. This was followed by a blocking step with 1% bovine serum albumin (BSA)/PBS at 37 °C for 5 min. After blocking, the cells were incubated with anti-osteocalcin (Abcam, 1:200 dilution), anti-osteopontin (Abcam, 1:200 dilution) or anti-BMP 2 (abcam, 1:200 dilution) for 1 h at 37 °C. The samples were then incubated with goat anti-rabbit IgG-HRP (1:200 dilution) at 4 °C for 30 min. After a final wash, the samples were mounted in hematoxylin to stain the nucleus. Images of the stained substrates were taken via a Leica IX71 microscope. Image J software was used for the data acquisition of staining intensity from the different substrates.

Immunofluorescence Staining

The localization of osteogenic markers OCN and BMP2 were analyzed by immunofluorescence staining. hBM-SCs culture on TCP, TMV and TMV-RGD1 coated substrates were terminated on 7 d and 14 d. Cells were fixed

with 4% formaldehyde in PBS containing 1% sucrose at 37 °C for 15 min. The fixative was then removed and the samples were permeabilized with 0.1% of Triton-X 100 at 4 °C for 10 min. This was followed by a blocking step with 1% bovine serum albumin (BSA)/PBS at 37 °C for 5 min. After blocking, the cells were incubated with anti-osteocalcin (Abcam, 1:200 dilution) or anti-BMP2 (Abcam, 1:200 dilution) in 1% BSA/PBS for 1 h at 37 °C. After that, Cy-3 conjugated secondary goat anti-rabbit antibody was used for 30 min at 4 °C. The samples were mounted in hoechst to stain the nucleus. Images of the stained substrates were taken via a Leica IX71 fluorescent microscope. Image J software was used for the data acquisition of staining intensity from the different substrates.

Alkaline Phosphatase (ALP) Activity

After 4 d, 7 d and 14 d of induction in the osteogenic media, the hBMSCs seeded on TCP and virus coated substrates were fixed with 4% formaldehyde for 15 min at room temperature. ALP activity was determined by incubating with BCIP/NBT (5-bromo-4-chloro-3-indolyl phosphate/nitroblue tetrazolium chloride) solution (Solarbio) at room temperature for 0.5 h according to the manufacturer's instruction. Images of the stained substrates were taken via a bright-field optical microscope. Image J software was used for the data acquisition to quantify the ALP activity.

Alizarin Red Staining

After 14 d of induction in the osteogenic media, hBM-SCs seeded on TCP and virus substrates were tested for Alizarin red staining to stain for calcium rich deposits. Cells were fixed in 4% formaldehyde for 15 min at room temperature. Then the cells were rinsed twice with ddH₂O followed by staining with 1% aqueous solution of Alizarin red (Duly) (pH 4.2) for 5 min in the dark. After rinse with ddH₂O and PBS, images of the stained substrates were taken by bright-field optical microscope. To quantify the amount of calcium deposition, 300 μ L of 0.1 M NaOH was added to each stained substrate to extract the dye from the samples. The absorbance of extracted dye solution was measured at 548 nm wavelength.

Oil Red O Staining

After 2 d, 5 d, 10 d and 15 d of induction in the adipogenic media, hBMSCs seeded on TCP and virus substrates were fixed with 4% formaldehyde and stained with oil red O solution for adipogenesis. Briefly, fixed cells were washed with PBS for three times, rinsed with 60% isopropanol and stained with Oil Red O (Sigma) in 60% isopropanol for 15 minutes. The cells were then rinsed with 60% isopropanol, and nuclei were stained with Mayer's Haematoxylin, then rinsed in PBS and cover-slipped with aqueous mounting medium. All stained samples were imaged using

a Leica IX71 microsystem. Image J software was used for the data acquisition to quantify the fat rate.

RESULTS AND DISCUSSION

Characterization of Virus-Coated Substrates

TMV-RGD1 is a mutant of wild type TMV by genetically inserting a cell adhesion motif, GRGDSPG. into the carboxyl end of TMV coat protein (Fig. 1(A)). The TMV-RGD1 mutant can keep its structural integrity and nanorod morphology as wild type TMV as shown in Figures 1(B) and (C). To obtain the stable coating of TMV and TMV-RGD1, PDL coated TCP was used as the underlying substrate. PDL is a positively charged biocompatible polymer which can strongly absorb the negatively charged viral particles (i.e., TMV particles) via electrostatic interaction. The TMV or TMV-RGD1 coating was fabricated by depositing viral particles on PDL coated substrates overnight. The presence of viral particles on substrates was analyzed by AFM. The AFM images showed a nearly complete coverage of substrates with TMV and TMV-RGD1 particles (Figs. 1(E and D)). The root mean square roughness (Rq) of virus substrates were collected from AFM images (n = 4), showing no significant difference of nanoscale roughness between TMV and TMV-RGD1 coating (Fig. 1(F)).

Cell Morphology and Cell Viability, 252.70.142 On: Mon

The hBMSCs were cultured on TCP, TMV and TMV-an Osteogenic Differentiation RGD1 coated substrates under osteogenic conditions and a To investigate the effect of various substrates on osteogenthe morphological differences of hBMSCs were imaged

during 14 days (data not shown). The hBMSCs were observed to attach and spread on all substrates after 6 h of incubation and continued to spread and proliferate significantly as the culture continued to 4 d and 7 d. After 14 d of incubation, the cells acquired a more spread morphology. There is no significant difference of hBMSCs morphology across the TCP and virus coated substrates, which is distinguished from the BMSCs derived from rats (rBMSCs) in previous reports. Compared to fully spread on TCP, the rBMSCs seeded on TMV substrates within 6 h showed partially spread but formed cell aggregates by 24 h after seeding.¹⁹ Similarly, rBMSCs aggregates on TMV-RGD1 was also observed after 48 h incubation.²²

The growth of hBMSCs on all substrates were determined by MTT assay (Fig. 2). No difference of cell numbers on various substrates was observed at 6 h after seeding. It was noted that cells cultured on TMV-RGD1 substrate showed a higher proliferation rate than that on TCP and TMV substrates at day 4. As the widely studied adhesive peptide, it is well-known that the RGD-peptide can promote the cell adhesion via the binding with integrin receptors, and consequently may upregulate the cell proliferation. 18,23 However, comparable cell proliferation rates were observed among TCP, TMV and TMV-RGD1 substrates as the culture continued to day 14. This is due to the fact that the later stage cell proliferation primarily relies on the secreted ECM proteins from adhered cells.

esis, the hBMSCs cultured on TCP, TMV and TMV-RGD1

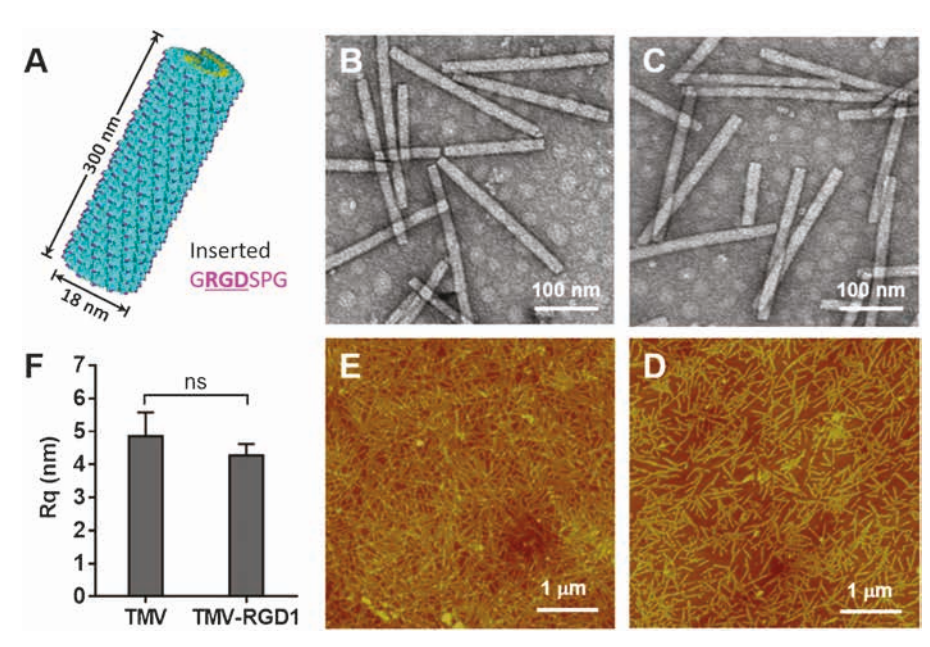


Figure 1. (A) Molecular model of TMV particle showing the surface display of RGD motif (pink). The model was generated using pymol with coordinate 2TMV from protein data bank. TEM images of (B) wild type TMV and its mutant (C) TMV-RGD1. AFM height images showing the coverage of PDL coated substrates with (E) TMV and (D) TMV-RGD1. (F) Root mean square roughness (Rq) of virus coated substrates. ns indicates nonsignificant and p > 0.05 based on student's t-test.

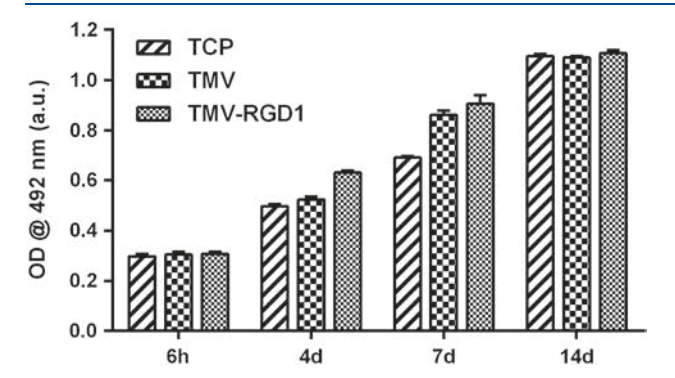


Figure 2. Proliferation of hBMSCs grown on the TCP and virus coated substrates for 6 h, 4 d, 7 d and 14 d, respectively.

substrates under osteogenic conditions were terminated at 6 h, 4 d, 7 d and 14 d. The changes in expression of osteogenic markers including OCN, RunX2, BMP2 and TGF-β were quantitatively assessed by RT-qPCR analysis (Fig. 3). OCN is the most specific marker for the osteogenic differentiation and mineralization, which is expressed during the post-proliferative period and reaches the maximum expression during mineralization.^{30,31} A significantly higher level of OCN expression was observed in the cells grown on TMV-RGD1 substrates at all other selected time points except 6 h, in comparison to those grown on TCP and TMV substrates. The highest level of OCN expression in cells on TMV-RGD1 occurred at 14 d

suggesting complete maturation of hBMSCs was expedited by TMV-RGD1. However, there was no significant difference of OCN expression between TMV and TCP substrates, which is in contrast to Kuar et al.'s study using rBMSCs. Significantly higher level of OCN was observed for rBMSCs cultured on TMV compared to that on TCP. RunX2 is an early specific marker and plays a vital role in osteogenic differentiation. The expression profile for RunX2 also showed a higher level in the cells cultured on TMV-RGD1 as compared to the TCP and TMV substrates.

BMP2 is known to be associated with stem cell differentiation.^{34,35} In rBMSCs cultured on virus substrate, osteogenic differentiation is mediated through the early up-regulation of BMP2 expression. 19,27 In our case, significantly higher levels of BMP2 were observed for hBM-SCs grown on TMV-RGD1 substrate by 14 d, which was decreased by increasing culture time to 28 d. Although a relatively higher expression level was observed in rBM-SCs cultured on TMV than that on TCP,16 there was no significant difference in the BMP2 expression for hBM-SCs cultured on TMV and TCP. TGF- β has been found to have a pivotal role in promoting osteoblast differentiation and bone formation depending on its concentration.^{36,37} In the beginning at 6 h, there was no difference on TGF- β expression among cells grown on different substrates. By day 4, the hBMSCs cultured on TMV-RGD1 substrate was noted to have significantly higher level of TGF- β expression in comparison of TCP control and

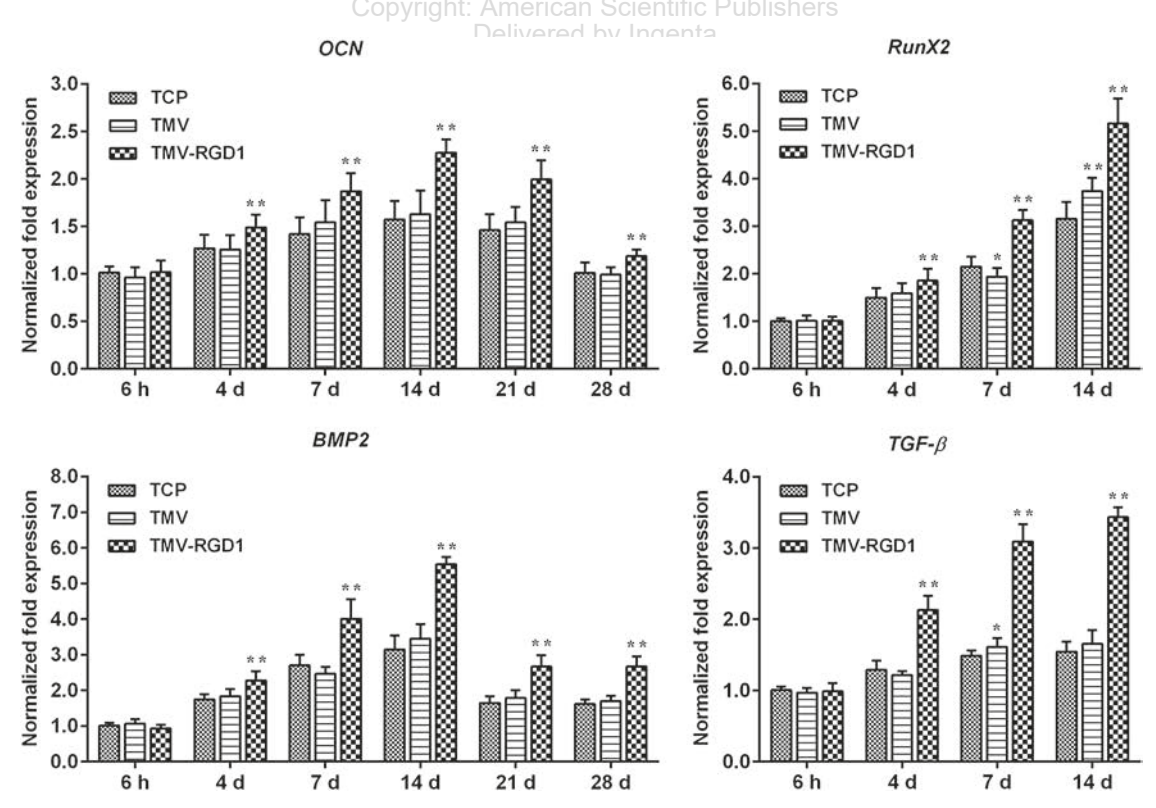


Figure 3. RT-qPCR analysis of osteogenic markers expression in hBMSCs cultured on TCP and virus coated substrates under osteogenic conditions for 6 h, 4 d, 7 d, 14 d, 21 d and 28 d. *p < 0.05 and **p < 0.01 based on one-way ANOVA.

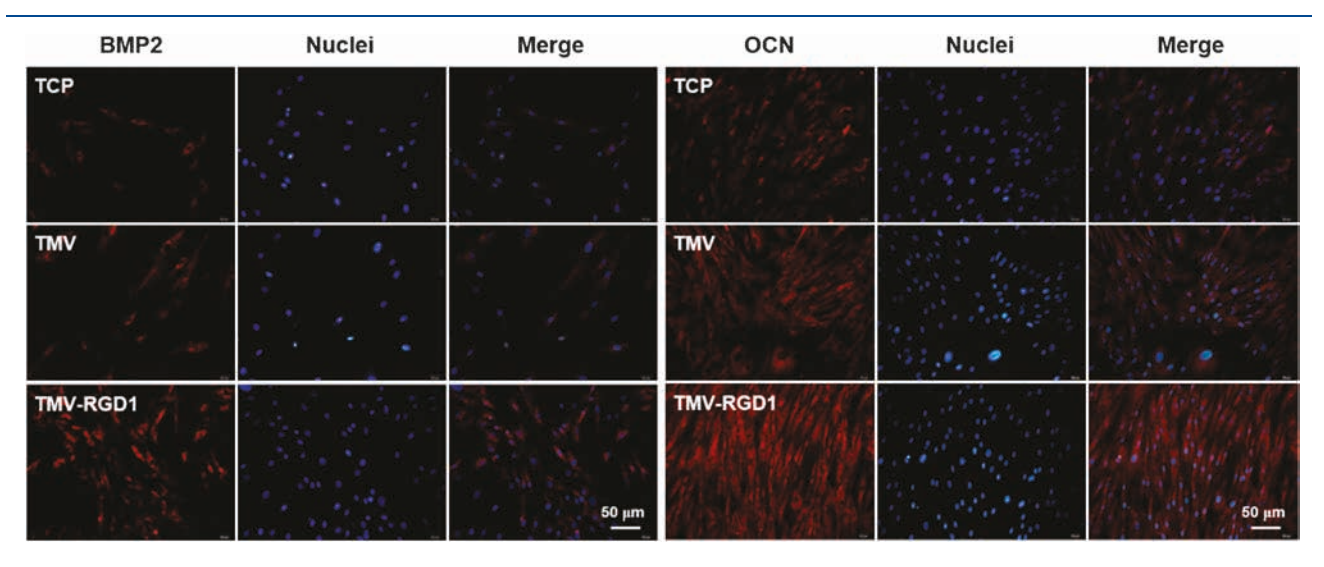


Figure 4. Representative images of immunofluorescence staining of BMP2 (7 d) and OCN (14 d) expression in hBMSCs cultured on TCP and virus coated substrates under osteogenic conditions.

TMV coated substrate. These gene expression profiles during osteogenesis implied that the nanoenvironment generated by TMV-RGD1 play a vital role in promoting the osteogenic differentiation of hBMSCs by up-regulating the expression of osteo-specific genes.

In order to assess if the difference observed in genomic level is translated at protein level, the hBMSCs grown on TCP and virus coated substrates under osteogenic conditions were analyzed for osteo-specific markers BMP2 and OCN expression by immunofluorescence staining (Fig. 4). The quantified BMP2 and OCN expression was analyzed as the fluorescence intensity and collected from immunostaining images (Fig. 5). In consistence with gene expression data, the immunofluorescence imaging of BMP2 revealed that hBMSCs cultured on TMV-RGD1 developed significantly higher levels of BMP2 expression at day 7 than those on TCP and TMV substrates. The highest level of OCN expression in cell cultures on TMV-RGD1 was observed at day 14 among all substrates. In addition, a slightly higher level of OCN expression was detected in cells grown on TMV than that on TCP.

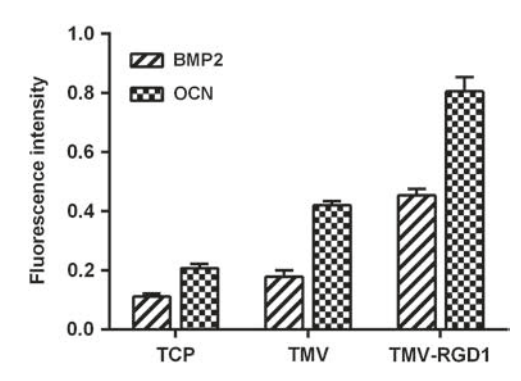


Figure 5. Quantified fluorescence intensity of BMP2 and OCN from immunofluorescence staining.

To determine the morphology change of hBMSCs during differentiation, cell cultures on various substrates were terminated at 6 h, 4 d and 7 d and cells were stained for osteo-specific markers OCN, OPN and BMP2 by immunohistochemical staining. As shown in Figure 6 hBMSCs cultured on all substrates revealed a wide spread morphology in the beginning at 6 h under osteogenic conditions and remained spread throughout the selected time points. The cells proliferated by the culture time increasing to day 4 and 7 for all substrates. It was noted that the cell densities on both TMV and TMV-RGD1 substrates at day 7 are slightly lower than that on TCP, which was due to the osteogenic differentiation induced by virus coated substrates. The expression of OCN, OPN and BMP2 in cells culture on all substrates was undetectable at 6 h. By increasing the culture time to day 4, detectable expression of OCN, OPN and BMP2 were observed in cells grown on all substrates. By day 7, a significantly increased expression of these three markers were noted in hBMSCs cultured on TMV-RGD1 substrate, in comparison to those on TCP and TMV substrates.

The enhancement in bone differentiation was also assessed by measuring ALP activity and calcium deposition at day 4, 7 and 14. ALP is an early marker of osteogenesis and its activity mediates matrix mineralization.³⁸ As shown in Figure 7, the ALP enzyme activity for all substrates showed a significant increase at day 7 and 14, in comparison to those at day 4. Over the course of 2 weeks, the hBMSCs culture on TMV-RGD1 substrate displayed significantly higher enzyme activity compared to the TCP and TMV substrates, suggesting that the TMV-RGD1 substrate improved the osteogenic differentiation of hBMSCs.

The calcium deposition is a critical step of osteogenesis and normally can be observed at the late stage of the process. Therefore, it was determined by staining with Alizarin Red S at day 14. As shown in Figure 8, small

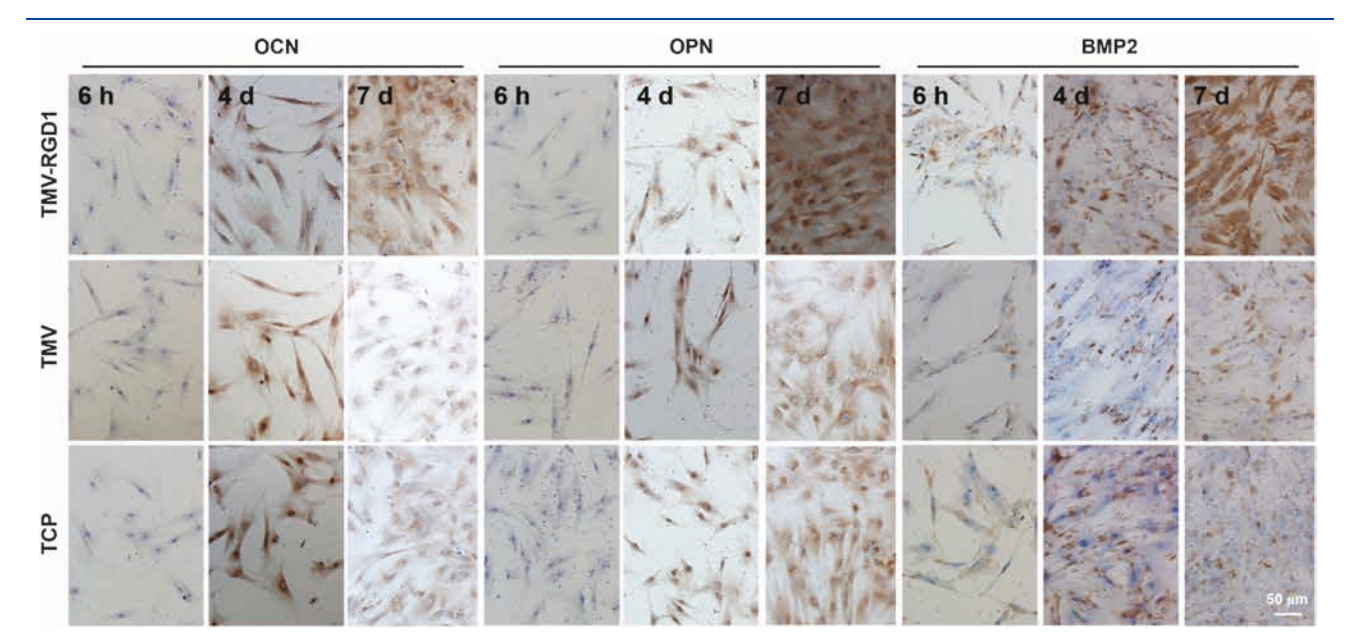


Figure 6. Representative photomicrographs of immunohistochemical staining of OCN, OPN and BMP2 in hBMSCs cultured on TCP and virus coated substrates under osteogenic conditions for 6 h, 4 d and 7 d.

nodules of mineralized calcium were observed for TCP control. The cells culture on TMV coated substrate showed a slightly more nodules compared to TCP, whereas the nodules were visibly larger for the cells grown on TMV-RGD1 coated substrate. UV-Vis absorbance measurements of the extracted dyes indicated that the cells on TMV and TMV-RGD1 substrates had significantly higher content of calcium in comparison to TCP control. It was noted that TMV-RGD1 induced the higher level of calcium deposition than TMV did, suggesting that TMV-RGD1 was more effective to enhance osteogenic differentiation and mineralization.

Adipogenic Differentiation

Many studies have revealed that there exists a reciprocal relationship between osteogenic and adipogenic

differentiation of MSCs that an osteogenic phenotype occurs at the expense of an adipogenic phenotype and vice versa.³⁹ As reported by Kilian et al., the hMSCs cultured on various shapes display different osteogenesis and adipogenesis profiles. They found that shapes promoting increased contractility led to preferential osteogenesis, whereas cells in shapes that promote low contractility preferred to follow an adipocyte lineage,⁴⁰ meaning that the osteogenesis and adipogenesis are opposite under a certain substrate.

To determine whether the virus coated substrates can mediate a similar response in hBMSCs, the hBMSCs were cultured on TMV and TMV-RGD1 coated substrates under adipogenic condition and stained with Oil Red O to probe the adipogenic differentiation. For adipogenesis, the phenotype of differentiation (as indicated by Oil red O

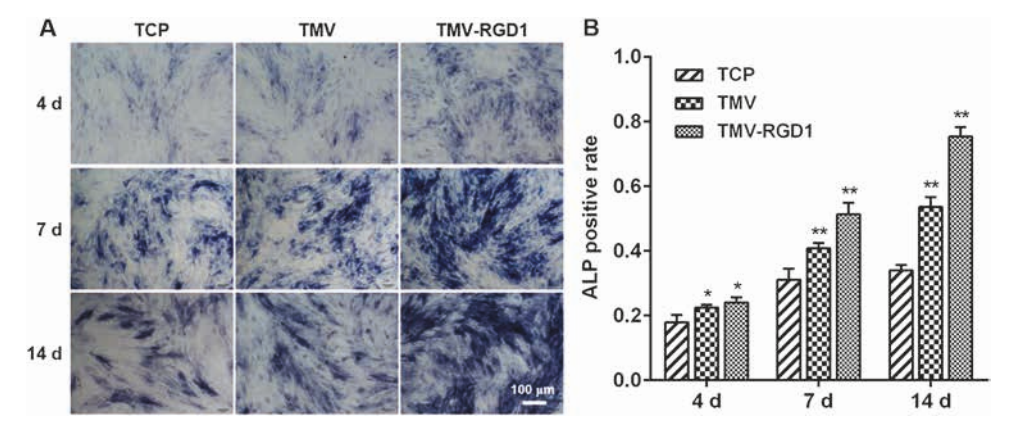


Figure 7. (A) Alkaline phosphatase staining of hBMSCs cultured on TCP and virus coated substrates under osteogenic conditions for 4 d, 7 d and 14 d. (B) Quantified alkaline phosphatase activity of hBMSCs collected from alkaline phosphatase staining images. *p < 0.05 and **p < 0.01 based on one-way ANOVA.

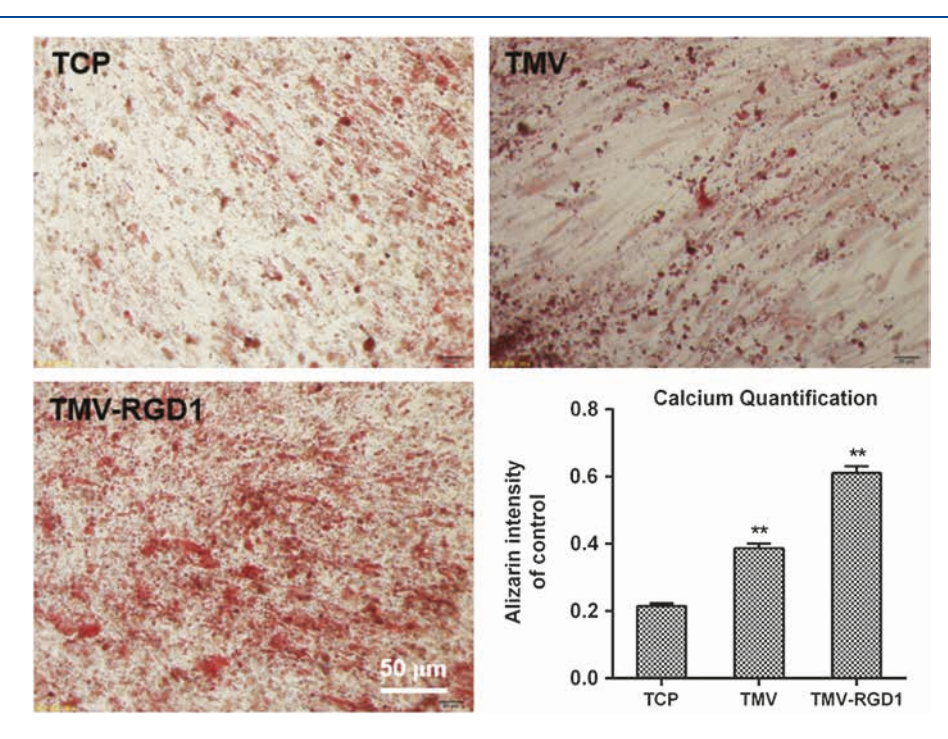


Figure 8. Alizarin red S staining and calcium quantification of hBMSCs cultured on TCP and virus coated substrates under osteogenic conditions for 14 d. **p < 0.01 based on one-way ANOVA.

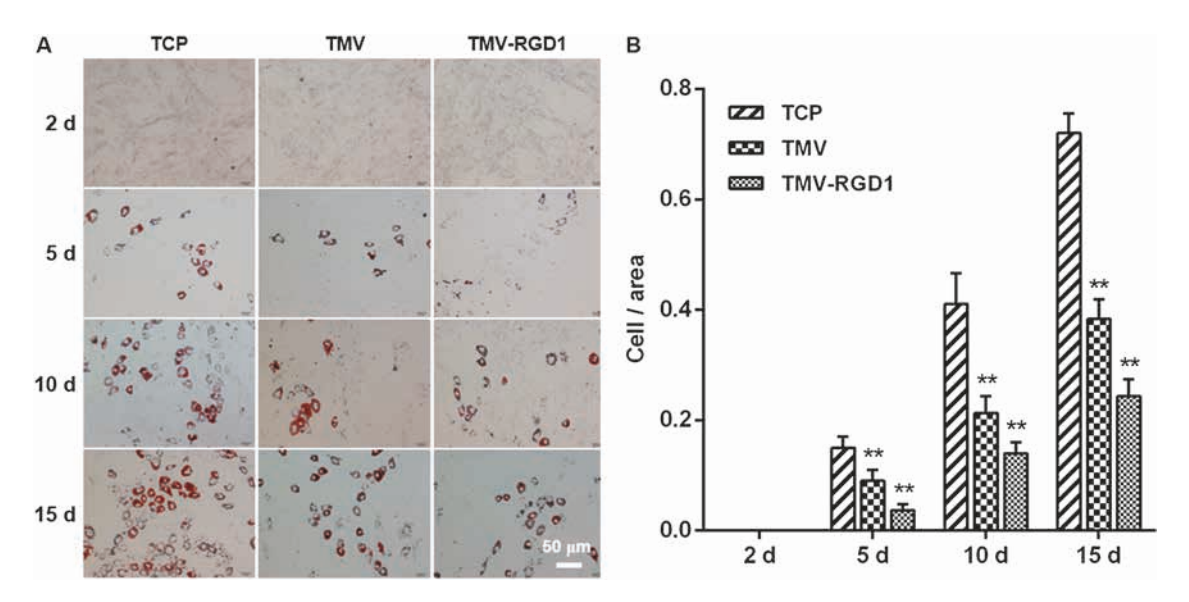


Figure 9. (A) Oil red O staining of hBMSCs cultured on TCP and virus coated substrates under adipogenic conditions. (B) Quantified hBMSCs that displayed lipid accumulation vacuoles. ** p < 0.01 based on one-way ANOVA.

staining) normally can be observed as early as 24–48 h, therefore, we started the measurement at day 2. As shown in Figure 9, Oil red O staining of the adipocytes cultured on TCP had a higher density of lipid droplets compared to TMV and TMV-RGD1 substrates. Clearly, the adipogenesis of hBMSCs was down-regulated on TMV and TMV-RGD1 coated substrates, which is consistent with literature report that a substrate if it could enhance the osteogenic

differentiation very often would decrease the adipogenic potential.

CONCLUSIONS

In the present study we have demonstrated that how the nanoenvironment generated by virus coating influence the differentiation pathways of hBMSCs. Although in this study no significant effect on osteogenic differentiation of hBMSCs was observed for TMV coating, our data indicated that the TMV-RGD1 substrate that bearing cell adhesion motifs significantly affected the expression levels of osteo-specific genes including OCN, RunX2, BMP2 and TGF- β in hBMSCs. The gene expression was further corroborated by immunostaining, which revealed the higher expression levels of OCN and BMP2 in cells on TMV-RGD1 substrate. Additionally, the subsequent cell differentiation was investigated by ALP activity assay and calcium deposition. On the other hand, the TMV coating impeded the adipogenic differentiation of hBMSCs significantly. All the data indicated that the TMV-RGD1 coating promoted the osteogenic differentiation of hBMSCs effectively in vitro. This can be attributed to two factors: (1) the interaction between RGD peptides and hBMSCs can enhance the cell adhesion and initial cell proliferation, and (2) the organization and clustering of RGD ligands on TMV can regulate the osteogenic differentiation as shown by Mooney and his coworker.⁴¹ Furthermore, as we demonstrated in our previous work, the virus-based scaffold may also contribute to the augmented osteogenesis due to the nanotopographic effects.^{27,42,43} Further investigation into the osteogenic effect of implants coated with TMV-RGD1 will be performed to better understanding this system and to apply it in clinical bone engineering applications.

Acknowledgments: Qian Wang would like to acknowledge the partial financial support from the NSF ECCS-1509076 and NSF OIA-1655740. We would like to acknowledge the technical support from Drs. Chenwei Zhang and Ying Wang from the Wuxi Puhe Biomedical Technology Co., Ltd.

REFERENCES

- M. F. Pittenger, A. M. Mackay, S. C. Beck, R. K. Jaiswal, R. Douglas, J. D. Mosca, M. A. Moorman, D. W. Simonetti, S. Craig, and D. R. Marshak, Multilineage potential of adult human mesenchymal stem cells. *Science* 284, 143 (1999).
- **2.** Y. L. Si, Y. L. Zhao, H. J. Hao, X. B. Fu, and W. D. Han, MSCs: Biological characteristics, clinical applications and their outstanding concerns. *Ageing Res. Rev.* 10, 93 (**2011**).
- J. Oswald, S. Boxberger, B. Jorgensen, S. Feldmann, G. Ehninger, M. Bornhauser, and C. Werner, Mesenchymal stem cells can be differentiated into endothelial cells in vitro. Stem Cells. 22, 377 (2004).
- L. da Silva Meirelles, P. C. Chagastelles, and N. B. Nardi, Mesenchymal stem cells reside in virtually all post-natal organs and tissues. J. Cell Sci. 119, 2204 (2006).
- S. J. Greco and P. Rameshwar, Microenvironmental considerations in the application of human mesenchymal stem cells in regenerative therapies. *Biologics*. 2, 699 (2008).
- B. Ohlstein, T. Kai, E. Decotto, and A. Spradling, The stem cell niche: Theme and variations. Curr. Opin. Cell Biol. 16, 693 (2004).
- G. Mendonca, D. B. Mendonca, F. J. Aragao, and L. F. Cooper, Advancing dental implant surface technology–from micron-to nanotopography. *Biomaterials* 29, 3822 (2008).
- M. J. Dalby, N. Gadegaard, R. Tare, A. Andar, M. O. Riehle, P. Herzyk, C. D. Wilkinson, and R. O. Oreffo, The control of human mesenchymal cell differentiation using nanoscale symmetry and disorder. *Nat. Mater.* 6, 997 (2007).

- B. G. Keselowsky, D. M. Collard, and A. J. Garcia, Integrin binding specificity regulates biomaterial surface chemistry effects on cell differentiation. *Proc. Natl. Acad. Sci. USA* 102, 5953 (2005).
- X. Zhao, Y. Lin, and Q. Wang, Virus-based scaffolds for tissue engineering applications. WIREs. Nanomed. Nanobiotechnol. 7, 534 (2015)
- 11. H. Zhu, B. Cao, Z. Zhen, A. A. Laxmi, D. Li, S. Liu, and C. Mao, Controlled growth and differentiation of MSCs on grooved films assembled from monodisperse biological nanofibers with genetically tunable surface chemistries. *Biomaterials* 32, 4744 (2011).
- J. Wang, L. Wang, X. Li, and C. Mao, Virus activated artificial ECM induces the osteoblastic differentiation of mesenchymal stem cells without osteogenic supplements. Sci. Rep. 3, 1242 (2013).
- 13. R. Gonzalez-McQuire, D. W. Green, K. A. Partridge, R. O. C. Oreffo, S. Mann, and S. A. Davis, Coating of human mesenchymal cells in 3D culture with bioinorganic nanoparticles promotes osteoblastic differentiation and gene transfection. *Adv. Mater.* 19, 2236 (2007).
- 14. W. F. Yang, L. Long, R. X. Wang, D. F. Chen, S. Duan, and F. J. Xu, Surface-modified hydroxyapatite nanoparticle-reinforced polylactides for three-dimensional printed bone tissue engineering scaffolds. J. Biomed. Nanotechnol. 14, 294 (2018).
- 15. J. Li, Y. Chen, N. Kawazoe, and G. Chen, Ligand density-dependent influence of arginine–glycine–aspartate functionalized gold nanoparticles on osteogenic and adipogenic differentiation of mesenchymal stem cells. *Nano Res.* 11, 1247 (2018).
- 16. G. Kaur, M. T. Valarmathi, J. D. Potts, E. Jabbari, T. Sabo-Attwood, and Q. Wang, Regulation of osteogenic differentiation of rat bone marrow stromal cells on 2D nanorod substrates. *Biomaterials* 31, 1732 (2010).
- 17. G. Kaur, C. Wang, J. Sun, and Q. Wang, The synergistic effects of multivalent ligand display and nanotopography on osteogenic differentiation of rat bone marrow stem cells. *Biomaterials* 31, 5813
- J. Luckanagul, L. A. Lee, Q. L. Nguyen, P. Sitasuwan, X. Yang, T. Shazly, and Q. Wang, Porous alginate hydrogel functionalized with virus as three-dimensional scaffolds for bone differentiation. *Biomacromolecules* 13, 3949 (2012).
- 19. P. Sitasuwan, L. A. Lee, P. Bo, E. N. Davis, Y. Lin, and Q. Wang, A plant virus substrate induces early upregulation of BMP2 for rapid bone formation. *Integr. Biol.* 4, 651 (2012).
- D. Borovsky, S. Rabindran, W. O. Dawson, C. A. Powell, D. A. Iannotti, T. J. Morris, J. Shabanowitz, D. F. Hunt, H. L. DeBondt, and A. DeLoof, Expression of Aedes trypsin-modulating oostatic factor on the virion of TMV: A potential larvicide. *Proc. Natl. Acad. Sci. USA* 103, 18963 (2006).
- 21. M. A. Bruckman, G. Kaur, L. A. Lee, F. Xie, J. Sepulveda, R. Breitenkamp, X. Zhang, M. Joralemon, T. P. Russell, T. Emrick, and Q. Wang, Surface modification of tobacco mosaic virus with "click" chemistry. *ChemBioChem.* 9, 519 (2008).
- 22. L. A. Lee, S. M. Muhammad, Q. L. Nguyen, P. Sitasuwan, G. Horvath, and Q. Wang, Multivalent ligand displayed on plant virus induces rapid onset of bone differentiation. *Mol. Pharm.* 9, 2121 (2012).
- 23. L. A. Lee, Q. L. Nguyen, L. Wu, G. Horvath, R. S. Nelson, and Q. Wang, Mutant plant viruses with cell binding motifs provide differential adhesion strengths and morphologies. *Biomacromolecules* 13, 422 (2012).
- 24. A. M. Osyczka, D. L. Diefenderfer, G. Bhargave, and P. S. Leboy, Different effects of BMP-2 on marrow stromal cells from human and rat bone. *Cells Tissues Organs* 176, 109 (2004).
- D. L. Diefenderfer, A. M. Osyczka, G. C. Reilly, and P. S. Leboy, BMP responsiveness in human mesenchymal stem cells. *Connect. Tissue Res.* 44(Suppl 1), 305 (2003).
- 26. G. C. Reilly, S. Radin, A. T. Chen, and P. Ducheyne, Differential alkaline phosphatase responses of rat and human bone marrow

- derived mesenchymal stem cells to 45S5 bioactive glass. *Biomaterials* 28, 4091 (2007).
- K. Metavarayuth, P. Sitasuwan, J. A. Luckanagul, S. Feng, and Q. Wang, Virus nanoparticles mediated osteogenic differentiation of bone derived mesenchymal stem cells. *Adv. Sci.* 2, 1500026 (2015).
- **28.** I. Lauria, C. Dickmeis, J. Roder, M. Beckers, S. Rutten, Y. Y. Lin, U. Commandeur, and H. Fischer, Engineered Potato virus X nanoparticles support hydroxyapatite nucleation for improved bone tissue replacement. *Acta Biomater.* **62**, 317 **(2017)**.
- 29. R. K. Silverwood, P. G. Fairhurst, T. Sjostrom, F. Welsh, Y. Sun, G. Li, B. Yu, P. S. Young, B. Su, R. M. Meek, M. J. Dalby, and P. M. Tsimbouri, Analysis of osteoclastogenesis/osteoblastogenesis on nanotopographical titania surfaces. Adv. Healthc. Mater. 5, 947 (2016).
- G. A. Rodan and M. Noda, Gene expression in osteoblastic cells. Crit. Rev. Eukaryot. Gene Expr. 1, 85 (1991).
- J. B. Lian and G. S. Stein, Concepts of osteoblast growth and differentiation: Basis for modulation of bone cell development and tissue formation. Crit. Rev. Oral Biol. Med. 3, 269 (1992).
- **32.** T. Komori, Requisite roles of Runx2 and Cbfb in skeletal development. *J. Bone Miner. Metab.* 21, 193 (**2003**).
- L. D. Carbonare, G. Innamorati, and M. T. Valenti, Transcription factor Runx2 and its application to bone tissue engineering. Stem Cell Rev. 8, 891 (2012).
- **34.** L. Wang, Y. Huang, K. Pan, X. Jiang, and C. Liu, Osteogenic responses to different concentrations/ratios of BMP-2 and bFGF in bone formation. *Ann. Biomed. Eng.* 38, 77 (**2010**).
- 35. T. Kawasaki, Y. Niki, T. Miyamoto, K. Horiuchi, M. Matsumoto, M. Aizawa, and Y. Toyama, The effect of timing in the

- administration of hepatocyte growth factor to modulate BMP-2-induced osteoblast differentiation. *Biomaterials* 31, 1191 (2010).
- **36.** K. S. Lee, S. H. Hong, and S. C. Bae, Both the Smad and p38 MAPK pathways play a crucial role in Runx2 expression following induction by transforming growth factor-beta and bone morphogenetic protein. *Oncogene* 21, 7156 (**2002**).
- 37. H. Zhang, M. Ahmad, and G. Gronowicz, Effects of transforming growth factor-beta 1 (TGF-beta1) on in vitro mineralization of human osteoblasts on implant materials. Biomaterials 24, 2013 (2003).
- W. Wang, D. Olson, B. Cheng, X. Guo, and K. Wang, Sanguis Draconis resin stimulates osteoblast alkaline phosphatase activity and mineralization in MC3T3-E1 cells. *J. Ethnopharmacol.* 142, 168 (2012).
- **39.** S. Lee, H. Y. Cho, H. T. Bui, and D. Kang, The osteogenic or adipogenic lineage commitment of human mesenchymal stem cells is determined by protein kinase C delta. *BMC Cell Biol.* 15, 42 (**2014**).
- K. A. Kilian, B. Bugarija, B. T. Lahn, and M. Mrksich, Geometric cues for directing the differentiation of mesenchymal stem cells. *Proc. Natl. Acad. Sci. USA* 107, 4872 (2010).
- K. Y. Lee, E. Alsberg, S. Hsiong, W. Comisar, J. Linderman, R. Ziff, and D. Mooney, Nanoscale adhesion ligand organization regulates osteoblast proliferation and differentiation. *Nano Lett.* 4, 1501 (2004).
- **42.** H. G. Nguyen, K. Metavarayuth, and Q. Wang, Upregulation of osteogenesis of mesenchymal stem cells with virus-based thin films. *Nanotheranostics* 2, 42 (**2018**).
- K. Metavarayuth, P. Sitasuwan, X. Zhao, Y. Lin, and Q. Wang, Influence of surface topographical cues on the differentiation of mesenchymal stem cells in vitro. ACS Biomater. Sci. Eng. 2, 142 (2016).

Copyright: American Scientific Publishers
Delivered by Ingenta